Supporting Information

First-principles study of electronic structure and point defects in higher manganese silicide Mn_4Si_7

Jun Chai,[a,†*] Guangshu Li,[b†] Mingping He[a], and Hangjia Shen[a]

[a]College of Chemical and Material Engineering, Quzhou University, Quzhou 324000, Zhejiang, China

[b]Key Laboratory of Solidification Control and Digital Preparation Technology (Liaoning Province), School of Materials Science and Engineering, Dalian University of Technology, Dalian 116024, China

[*]Corresponding authors. E-mail address: chaijun@qzc.edu.cn (Jun Chai).

[†]These authors contributed equally to this work.

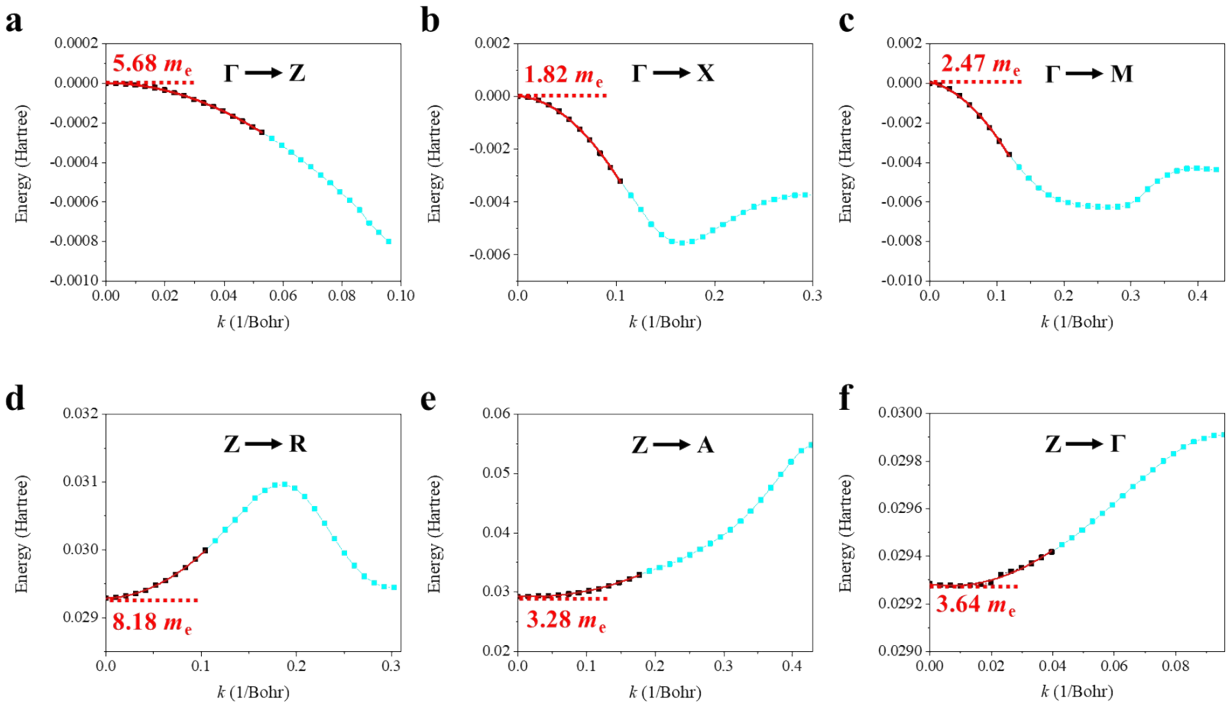

Fig. S1 The effective masses of hole and electron carriers at VBM (a, b, c) and CBM (d, e, f) for Mn_4Si_7 were evaluated along different directions. The black points near VBM and CBM are fitted using a quadratic term $y = A+Bx+Cx^2$. The red line represents the fitting result, where the effective mass is given by $\frac{1}{2C}m_e$.

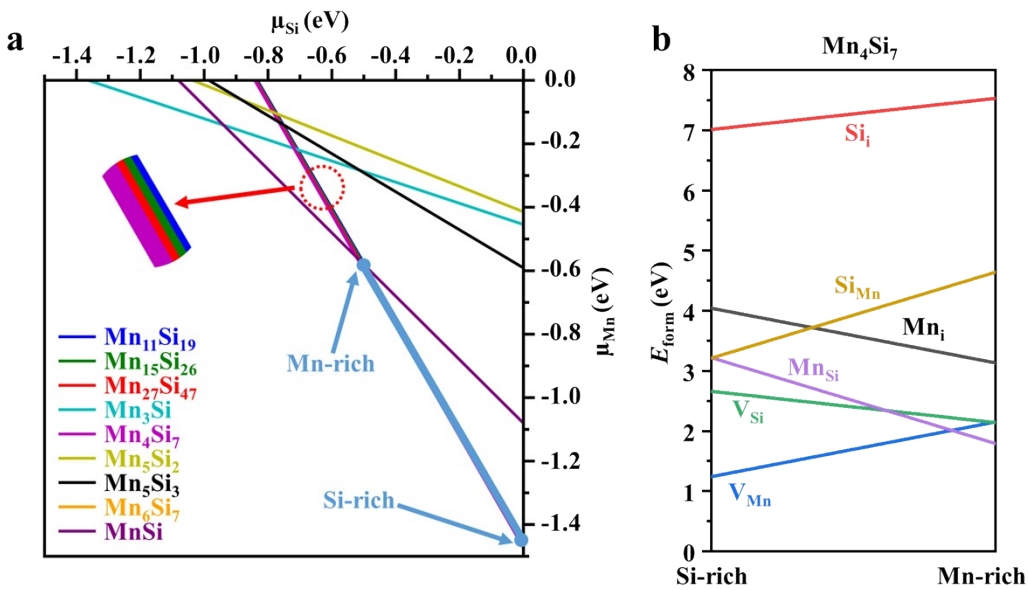

Fig. S2 (a) The calculated stable region of Mn_4Si_7 in the chemical potential space spanned by μ_{Mn} and μ_{Si}. Each straight line corresponds to $x\ \mu_{Mn} + y\ \mu_{Si} = \Delta H(Mn_xSi_y)$. The allowed region is delineated by a bold blue line. The inset, magnifying the area within the red circle, illustrates the constituted compounds of HMS, namely Mn_4Si_7, $Mn_{11}Si_{19}$, $Mn_{15}Si_{26}$ and $Mn_{27}Si_{47}$. (b) The formation energies of the intrinsic point defects in Mn_4Si_7 as a function of chemical potentials between the Si-rich and Mn-rich conditions. These results are obtained using the PBEsol functional**.**

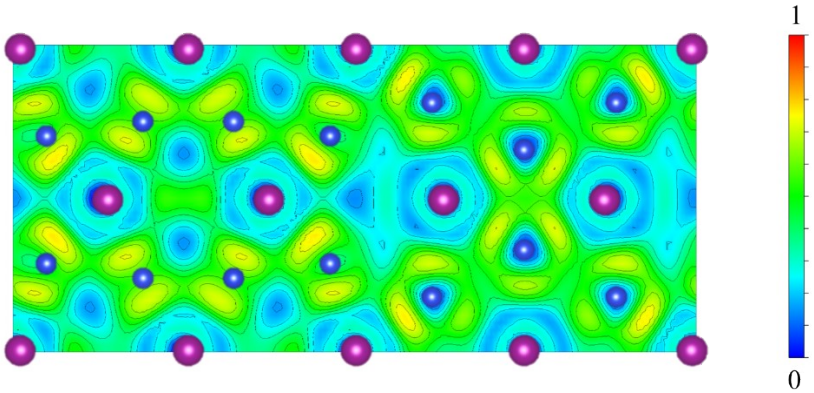

Fig. S3 Two-dimensional Electron Localization Function (ELF) contour plots on (110) plane of Mn_4Si_7 in Fig. 1. Mn and Si atoms are represented by purple and blue spheres. The contour lines are spaced at intervals of 0.08. The closer the ELF is to zero, the more ionic the bonding features.

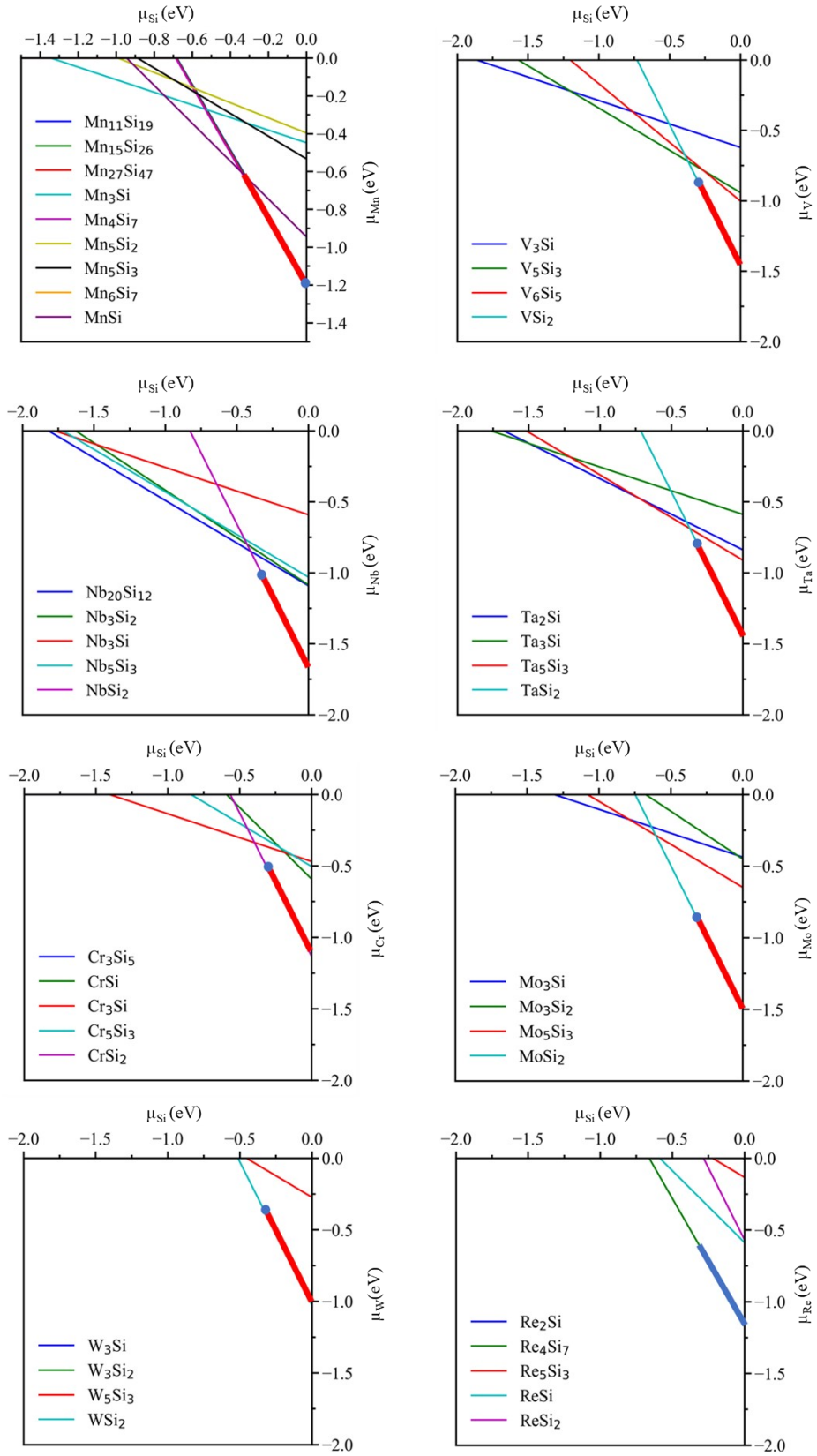
μSi (eV)
μMn (eV)
Mn11Si19
Mn15Si26
Mn27Si47
Mn3Si
Mn4Si7
Mn5Si2
Mn5Si3
Mn6Si7
MnSi
μV (eV)
V3Si
V5Si3
V6Si5
VSi2
μNb (eV)
Nb20Si12
Nb3Si2
Nb3Si
Nb5Si3
NbSi2
μTa (eV)
Ta2Si
Ta3Si
Ta5Si3
TaSi2
μCr (eV)
Cr3Si5
CrSi
Cr3Si
Cr5Si3
CrSi2
μMo (eV)
Mo3Si
Mo3Si2
Mo5Si3
MoSi2
μW (eV)
W3Si
W3Si2
W5Si3
WSi2
μRe (eV)
Re2Si
Re4Si7
Re5Si3
ReSi
ReSi2

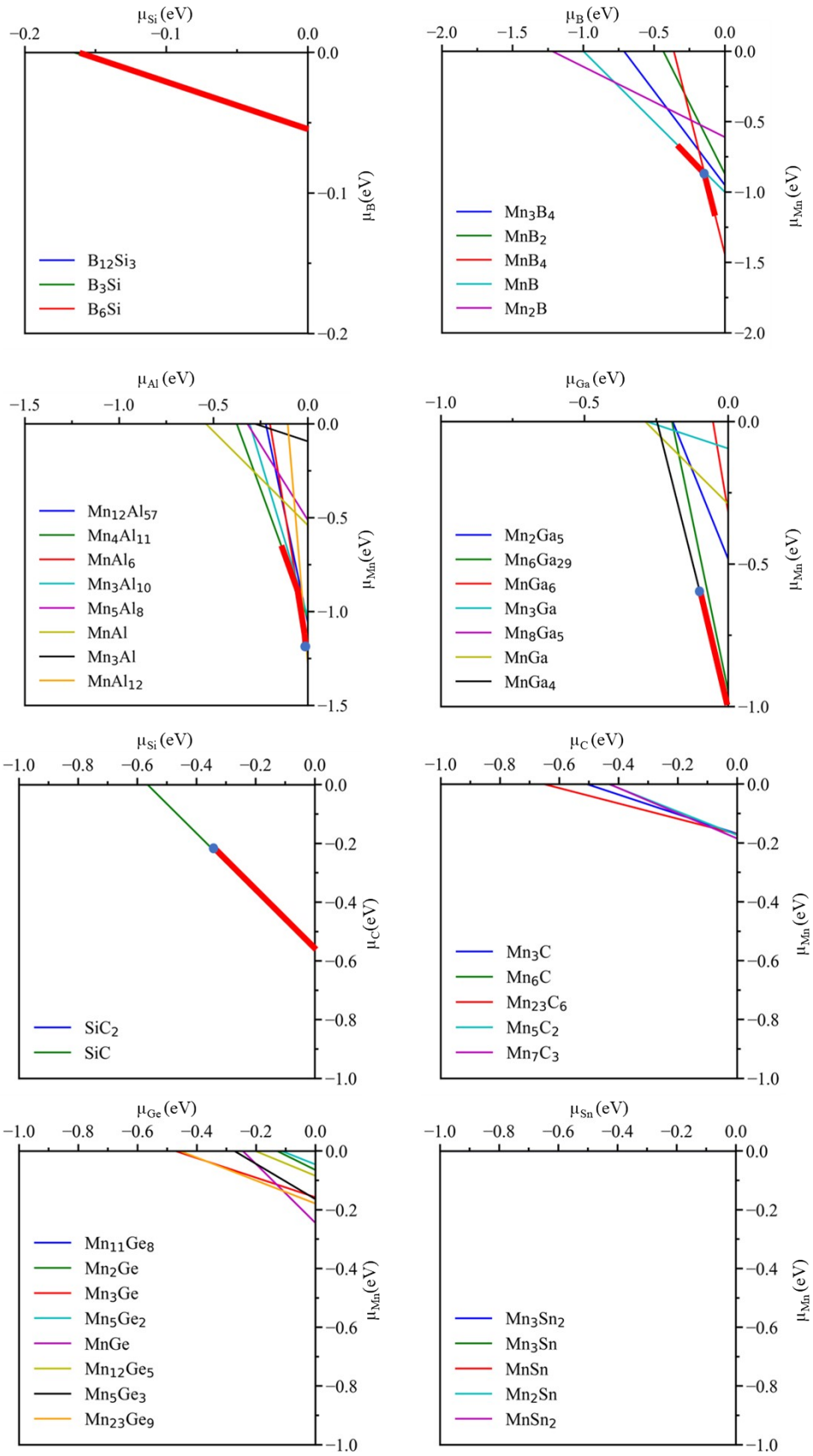
μSi (eV)
μB (eV)
B12Si3
B3Si
B6Si
μB (eV)
μMn (eV)
Mn3B4
MnB2
MnB4
MnB
Mn2B
μAl (eV)
μMn (eV)
Mn12Al57
Mn4Al11
MnAl6
Mn3Al10
Mn5Al8
MnAl
Mn3Al
MnAl12
μGa (eV)
μMn (eV)
Mn2Ga5
Mn6Ga29
MnGa6
Mn3Ga
Mn8Ga5
MnGa
MnGa4
μSi (eV)
μC (eV)
SiC2
SiC
μC (eV)
μMn (eV)
Mn3C
Mn6C
Mn23C6
Mn5C2
Mn7C3
μGe (eV)
μMn (eV)
Mn11Ge8
Mn2Ge
Mn3Ge
Mn5Ge2
MnGe
Mn12Ge5
Mn5Ge3
Mn23Ge9
μSn (eV)
μMn (eV)
Mn3Sn2
Mn3Sn
MnSn
Mn2Sn
MnSn2

Fig. S4 Determination of the allowed region for chemical potentials. Each straight line corresponds to $x\ \mu_{Mn} + y\ \mu_{Si} = \Delta H(Mn_xSi_y)$, $x\ \mu_D + y\ \mu_{Si} = \Delta H(D_xSi_y)$, and $x\ \mu_{Mn} + y\ \mu_D = \Delta H(Mn_xD_y)$. Mn_xSi_y, D_xSi_y, and Mn_xD_y represent the Mn-Si binary compounds, *D*-Si binary compounds, and Mn-*D* binary compounds, respectively. ΔH is the calculated enthalpy of formation. The thick solid red lines mark the allowed chemical potential regions and the blue dots indicate the condition used for obtaining Fig. 5, at which the corresponding formation energy is the lowest. It is worth noting that the straight lines for binary compounds with $\Delta H > 0$ will not be displayed.

Table S1 Total magnetization for Mn_4Si_7 containing intrinsic defects.

Defect type	Total magnetization (μ_B)
V_{Mn} ($Mn_{63}Si_{112}$)	0.99
V_{Si} ($Mn_{64}Si_{111}$)	3.71
Mn_i ($Mn_{65}Si_{112}$)	3.03
Si_i ($Mn_{64}Si_{113}$)	4.00
Mn_{Si} ($Mn_{65}Si_{111}$)	3.01
Si_{Mn} ($Mn_{63}Si_{113}$)	0.59

Table S2 The charge state of Mn and Si for Mn_4Si_7 obtained by using Bader charge analysis. The lattice constants are $a = b = 5.498$ Å and $c = 17.35$ Å.

Atom	*x*	*y*	*z*	Charge state
Mn1	0.000000	0.000000	0.250000	0.12
Mn2	0.000000	0.000000	0.750000	-0.01
Mn3	0.000000	0.000000	0.000000	-0.21
Mn4	0.000000	0.000000	0.500000	-0.21
Mn5	0.500000	0.500000	0.130090	-0.19
Mn6	0.500000	0.500000	0.869910	-0.21
Mn7	0.500000	0.500000	0.630090	-0.21
Mn8	0.500000	0.500000	0.369910	-0.19
Mn9	0.000000	0.500000	0.065081	-0.11
Mn10	0.500000	0.000000	0.934919	-0.10
Mn11	0.000000	0.500000	0.565081	-0.10
Mn12	0.500000	0.000000	0.434919	-0.11
Mn13	0.000000	0.500000	0.308212	-0.05
Mn14	0.500000	0.000000	0.691788	-0.10
Mn15	0.000000	0.500000	0.808212	-0.10
Mn16	0.500000	0.000000	0.191788	-0.05
Si1	0.345942	0.769431	0.038804	0.07
Si2	0.654058	0.230569	0.038804	0.14
Si3	0.769431	0.654058	0.961196	0.09
Si4	0.230569	0.345942	0.961196	0.10
Si5	0.345942	0.230569	0.538804	0.05
Si6	0.654058	0.769431	0.538804	0.14
Si7	0.769431	0.345942	0.461196	0.11
Si8	0.230569	0.654058	0.461196	0.11
Si9	0.199407	0.155412	0.112824	-0.03
Si10	0.800592	0.844588	0.112824	0.04
Si11	0.155412	0.800592	0.887176	0.05
Si12	0.844588	0.199407	0.887176	0.03

Si13	0.199407	0.844588	0.612824	0.02
Si14	0.800592	0.155412	0.612824	0.05
Si15	0.155412	0.199407	0.387176	0.02
Si16	0.844588	0.800592	0.387176	-0.01
Si17	0.158878	0.678921	0.182512	0.05
Si18	0.841122	0.321079	0.182512	-0.03
Si19	0.678921	0.841122	0.817488	-0.01
Si20	0.321079	0.158878	0.817488	0.08
Si21	0.158878	0.321079	0.682512	0.07
Si22	0.841122	0.678921	0.682512	0.00
Si23	0.678921	0.158878	0.317488	0.04
Si24	0.321079	0.841122	0.317488	-0.03
Si25	0.333920	0.333920	0.250000	0.08
Si26	0.666080	0.666080	0.250000	0.25
Si27	0.333920	0.666080	0.750000	0.10
Si28	0.666080	0.333920	0.750000	0.23

Table S3 Binary compounds of Mn-Si-*D* systems which are used in determining the chemical potentials for calculating defect formation energy. All structures are obtained from ICSD.

Mn-Si	$Mn_{11}Si_{19}$ ($P4_1cd$ #110), $Mn_{15}Si_{26}$ (I-4_2d #122), $Mn_{27}Si_{47}$ ($P4_1cd$ #110), Mn_3Si (Fm-3m #225), Mn_4Si_7 (P-4c2 #116), Mn_5Si_2 ($P4_12_12$ #92), Mn_5Si_3 ($P2_1$/m #11, Cmcm #63, $P6_3$/mcm #193), Mn_6Si_7 (R-3m #166), MnSi ($P2_13$ #198)
V-Si **Mn-V**	V_3Si (Pm-3n #223), V_5Si_3 ($P6_3$/mcm #193, I4/mcm #140), V_6Si_5 (Immm #71, Ibam #72), VSi_2 ($P6_222$ #180)
Nb-Si **Mn-Nb**	Nb_3Si_2 (P4/mbm #127), Nb_3Si (Pm-3n #223, Pm-3m #221, $P4_2$/n #86), Nb_5Si_3 (I4/mcm #140, $P6_3$/mcm #193), $NbSi_2$($P6_222$ #180)
Ta-Si **Mn-Ta**	Ta_2Si (I4/mcm #140), Ta_3Si ($P4_2$/n #86), Ta_5Si_3 ($P6_3$/mcm #193, I4/mcm #140), $TaSi_2$ ($P6_222$ #180)
Cr-Si **Mn-Cr**	Cr_3Si (Pm-3n #223), Cr_3Si_5 (I4/mcm #140), Cr_5Si_3 (I4/mcm #140), CrSi ($P2_13$ #198), $CrSi_2$ ($P6_222$ #180, I4/mmm#139)
Mo-Si **Mn-Mo**	Mo_3Si (Pm-3n #223), Mo_3Si_2 (P4/mbm #127), Mo_5Si_3 (I4/mcm #140, P63/mcm #193), $MoSi_2$ ($P6_222$ #180, I4/mmm#139)
W-Si **Mn-W**	W_3Si (Pm-3n #223) W_3Si_2 (P4/mbm #127), W_5Si_3 (I4/mcm #140), WSi_2 ($P6_222$ #180, I4/mmm#139)
Re-Si **Mn-Re**	Re_2Si ($P2_1$/c #14), Re_4Si_7 (Cm #8), Re_5Si_3 (I4/mcm #140), ReSi ($P2_13$ #198), $ReSi_2$ (I4/mmm #139, Immm #71)
B-Si **Mn-B**	$B_{12}Si_3$ (R-3m #166), B_3Si (Imma #74), B_6Si (Pm-3m #221) MnB (Pnma #62, $P4_2$/ncm, #138), Mn_2B (I4/mcm #140), MnB_2 (P6/mmm #191), MnB_4 (Pnnm #58, C2/m #12, P21/c #14), Mn_3B_4 (Immm #71)

Al-Si	Al_8Si_{38} (P1 #1)
Mn-Al	MnAl (P4/mmm #123), Mn_3Al (F-43m #216), Mn_3Al_{10} ($P6_3$/mmc #194), Mn_4Al_{11} (P-1 #2), $MnAl_{12}$ (Im-3 #204), $Mn_{12}Al_{57}$ (Pm-3 #200), $MnAl_6$ (Cmcm #63), Mn_5Al_8 (R3m #160)
Ga-Si	MnGa (P4/mmm #123, R-3m #166), Mn_3Ga (Fm-3m #225, $P6_3$/mmc #194), Mn_6Ga_{29} (P-1 #2), $MnGa_4$ (Im-3m #229), Mn_2Ga_5 (P4/mbm #127), Mn_8Ga_5 (I-43m #127), $MnGa_6$ (Cmcm #63)
Mn-Ga	
In-Si	None
Mn-In	
C-Si	SiC (F-43m #216, Fm-3m #225, P3m1 #156, $P6_3$/mc #186, R3m #160), SiC_2 ($P4_2$/mmc #131, Pa-3 #205)
Mn-C	Mn_3C (Pnma #62), Mn_6C (Fd-3m #227), $Mn_{11}C_3$ (F23 #196), Mn_5C_2 (C2/c #15), Mn_7C_3 (Pnma #62), $Mn_{23}C_6$ (Fm-3m #225)
Ge-Si	MnGe ($P2_12_12_1$ #19, $P2_13$ #198), Mn_2Ge(F-43m #216, $P6_3$/mmc #194), Mn_3Ge (Pm-3m #221, Fm-3m #225, $P6_3$/mmc #194), Mn_5Ge_2 (Ibam #72, P3c1 #158), Mn_5Ge_3 ($P6_3$/mcm #193), $Mn_{12}Ge_5$ (R32 #155), $Mn_{11}Ge_8$ (Pnma #62), $Mn_{23}Ge_9$ (P3c1 #158)
Mn-Ge	
Sn-Si	MnSn (Pm-3m #221, Fm-3m #225, $P6_3$/mmc #194, F-43m #216), $MnSn_2$ (I4/mcm #140), Mn_2Sn ($P6_3$/mmc #194), Mn_3Sn ($P6_3$/mmc #194, Fm-3m #225), Mn_3Sn_2 (Pnma #62)
Mn-Sn	

Table S4 Total magnetization for Mn_4Si_7 containing extrinsic defects.

Dopant type	Total magnetization (μ_B)
None ($Mn_{16}Si_{28}$)	0
V ($Mn_{15}VSi_{28}$)	1.73
Nb ($Mn_{15}NbSi_{28}$)	0.00
Ta ($Mn_{15}TaSi_{28}$)	0.00
Cr ($Mn_{15}CrSi_{28}$)	0.97
Mo ($Mn_{15}MoSi_{28}$)	0.98
W ($Mn_{15}WSi_{28}$)	0.93
Re ($Mn_{15}ReSi_{28}$)	0.00
B ($Mn_{16}Si_{27}B$)	0.91
Al ($Mn_{16}Si_{27}Al$)	0.72
Ga ($Mn_{16}Si_{27}Ga$)	0.66
In ($Mn_{16}Si_{27}In$)	0.91
C ($Mn_{16}Si_{27}C$)	0.00
Ge ($Mn_{16}Si_{27}Ge$)	0.00
Sn ($Mn_{16}Si_{27}Sn$)	0.00

Table S5 The maximum ELF value for Mn_4Si_7 containing extrinsic defects.

Dopant type	ELF value
None ($Mn_{16}Si_{28}$)	0.834
V ($Mn_{15}VSi_{28}$)	0.664
Nb ($Mn_{15}NbSi_{28}$)	0.668
Ta ($Mn_{15}TaSi_{28}$)	0.668
Cr ($Mn_{15}CrSi_{28}$)	0.670
Mo ($Mn_{15}MoSi_{28}$)	0.657
W ($Mn_{15}WSi_{28}$)	0.679
Re ($Mn_{15}ReSi_{28}$)	0.673
B ($Mn_{16}Si_{27}B$)	0.670
Al ($Mn_{16}Si_{27}Al$)	0.668
Ga ($Mn_{16}Si_{27}Ga$)	0.670
In ($Mn_{16}Si_{27}In$)	0.665
C ($Mn_{16}Si_{27}C$)	0.679
Ge ($Mn_{16}Si_{27}Ge$)	0.678
Sn ($Mn_{16}Si_{27}Sn$)	0.670